Supplementary information

Tunable Au core-Ag shell nanoparticle tip for tip-enhanced spectroscopy

Woong Kim[1†], Nara Kim[2†], Eunbyoul Lee[3▽], Duckhoe Kim[1‡], Zee Hwan Kim[2]*

and Joon Won Park[1]*

1. Department of Chemistry, Pohang University of Science and Technology, San 31 Hyoja-dong, Pohang, 790-784, Korea

2. Department of Chemistry, Seoul National University, Seoul 151-742, Korea

3. Department of Chemistry, Korea University, Seoul 136-701, Korea

Corresponding Author

Zee Hwan Kim, Department of Chemistry, Seoul National University, Seoul, 151-742, Korea.

E-mail: zhkim@snu.ac.kr

Joon Won Park, Department of Chemistry, Pohang University of Science and Technology, San 31 Hyoja-dong, Pohang, 790-784, Korea.

E-mail: jwpark@postech.ac.kr

Author Contributions

† These authors contributed equally.

▽ Current address: Doosan Corporation Electro-Materials, Sujigu, Gyeonggi –do, Korea.

‡ Current address: The Department of Biological Sciences, Columbia University, New York, USA.

1. Single seed nanoparticle attached probe

Figure S1 shows the transfer process of a single seed AuNP through the different unbinding force values between short DNA and long one. A 63 bp DNA strand tethering the seed AuNP was hybridized with a 20 bp DNA strand immobilized on the silicon wafer surface. An atomic force microscopy (AFM) tip (Contact-G, BudgetSensors) tethering a 40 bp DNA strand was controlled to approach the substrate. At the tip-sample contact, the 40 bp DNA on the tip was hybridized with the complementary part of the 63 bp DNA strand captured by the 20 bp strand. The binding force between the former two strands (40 bp and 63 bp DNAs) is stronger than that between the other two (20 bp and 63 bp DNAs). Therefore, the 63 bp DNA (AuNP) was transferred from the substrate to end of the tip upon retraction.

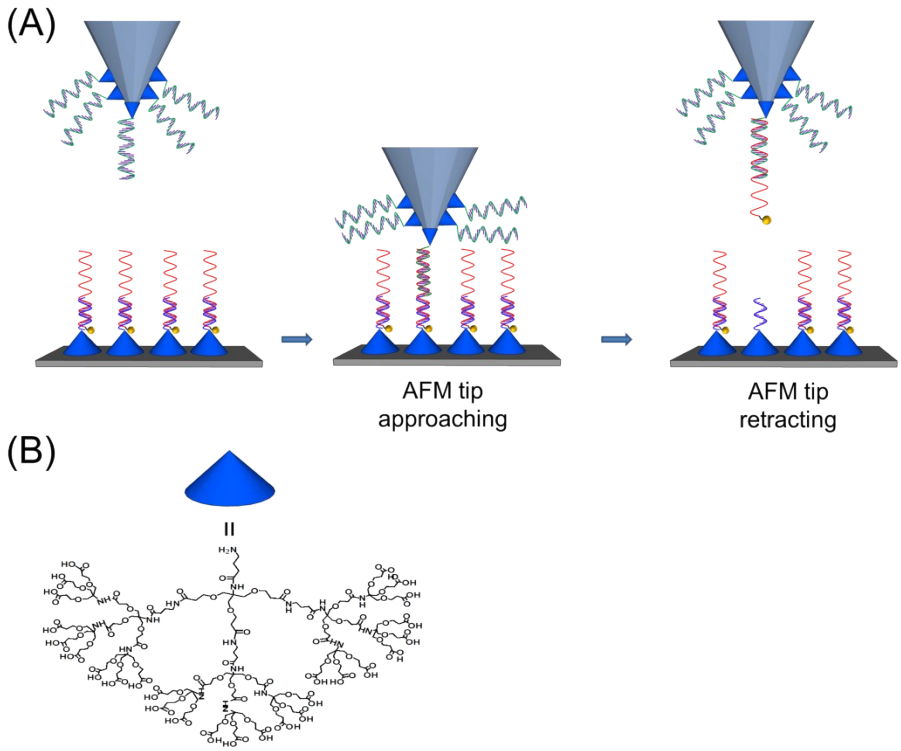

Figure S1. (A) A scheme illustrating the transfer of a single DNA strand tethering a seed AuNP from the substrate to the end of the tip. (B) Chemical structure of the dendron used for the substrate and tip modification.

2. Characteristics of AFM tip (BudgetSensors, Contact-G)

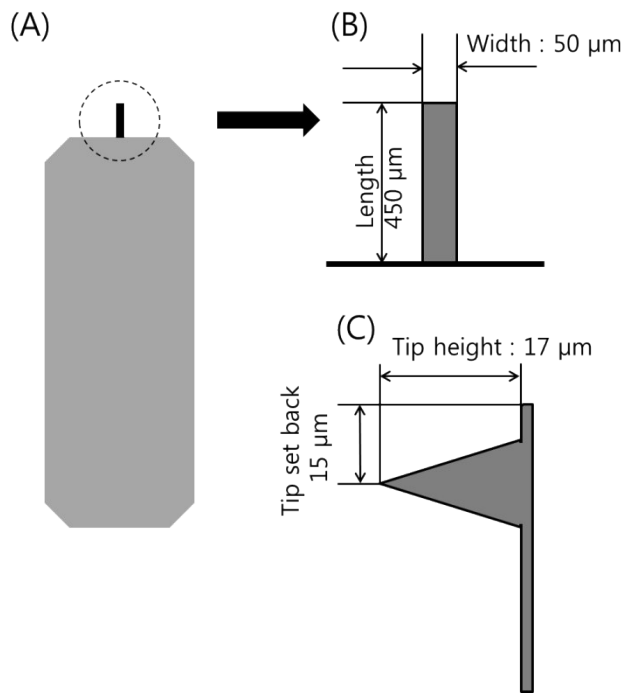

(D)

	Typical values
Resonant frequency	13 kHz
Spring constant	0.2 N/m
Cantilever length	450 μm
Mean width	50 μm
Tip height	17 μm
Tip set back	15 μm
Tip radius	< 10 nm
Backside coating	none
Material	Si

Figure S2. Characteristics of the employed AFM tip (BudgetSensors, Contact-G). (A) A top view of the AFM chip. (B) Diameter and width of the cantilever. (C) A side view showing tip height and set back. (D) A table for other information.

3. TERS set-up

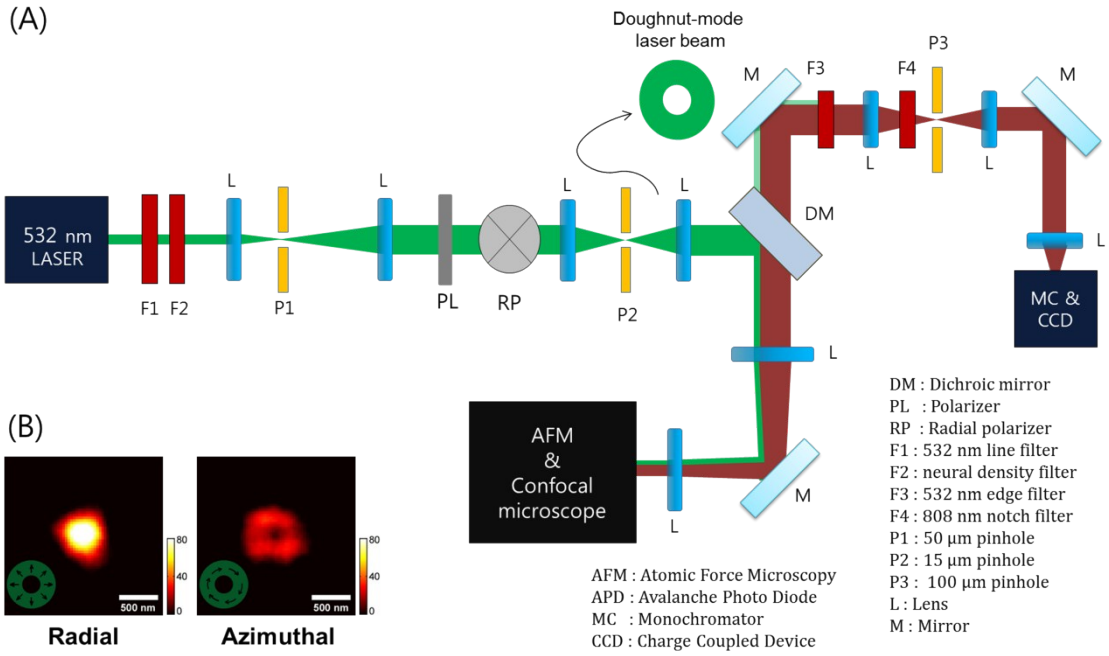

Figure S3. (A) Overall experimental set-up. (B) Confocal fluorescence images of a fluorescent bead (diameter of 20 nm) on a glass coverslip obtained with a radially polarized laser beam and an azimuthally polarized laser beam (532 nm). In the experiments described in the main text, the radially polarized laser beam is used to enhance the z-polarized (perpendicular to the sample surface and parallel to the main axis of the tip) electric field component.

4. Measurement of Au@Ag nanoparticle size

Au core-Ag shell nanoparticles are not spherical; the shape is different for each case, even for similarly sized particles. In addition to the shape variation, the orientation and position can vary. The *effective* diameter of the NP is the total length projected on the sample (xy) plane. When the length was calculated from the corresponding TEM image, precisely finding the perpendicular axis was difficult. Therefore, a range of lengths was obtained as best estimates, and the estimated values were averaged. The error bar represents the standard deviation of the values.

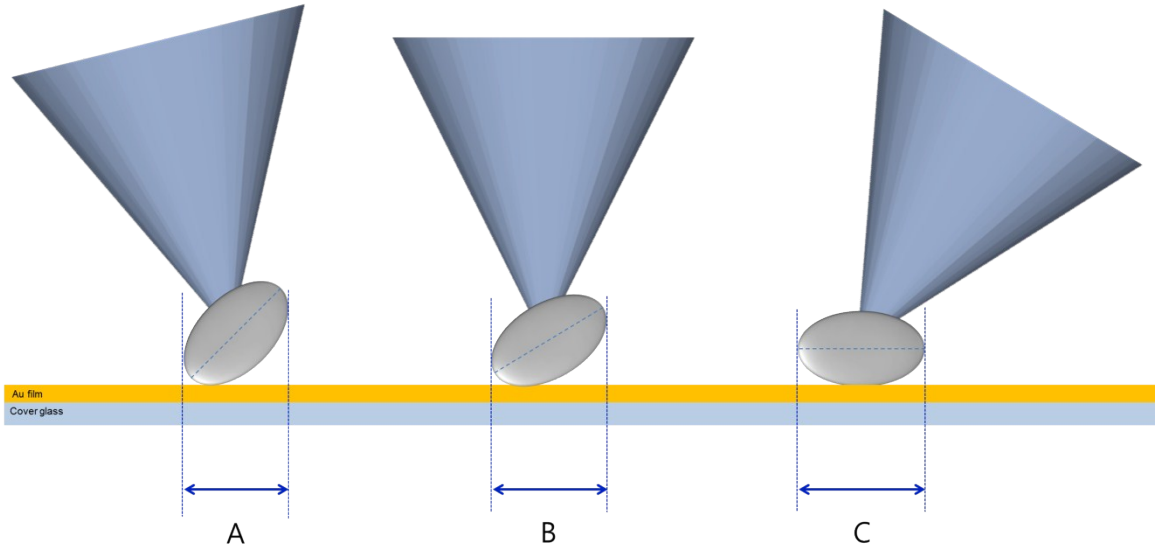

Figure S4. Examples of various effective diameters of an elliptical nanoparticle.

5. Raman spectroscopy of biphenyl-4-thiol

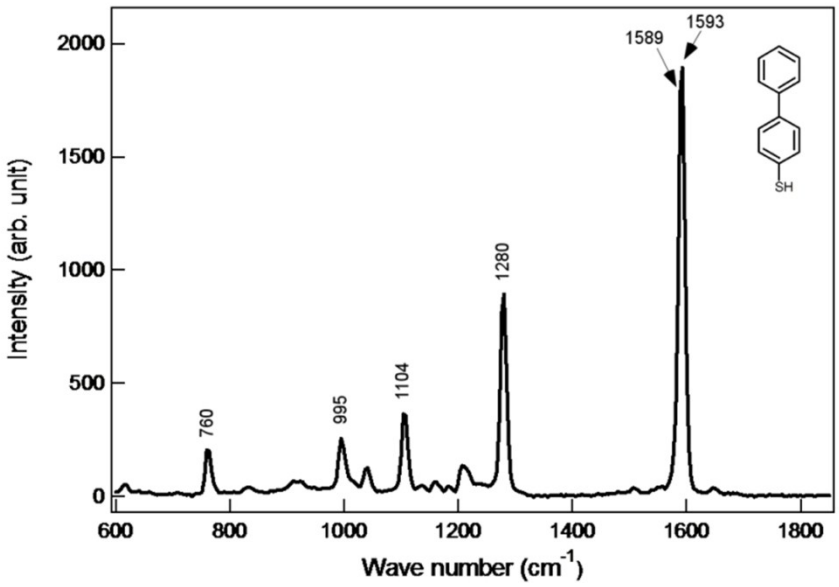

Figure S5. Normal Raman spectrum of biphenyl-4-thiol (powder).

6. Experimental estimation of enhancement factors

The Raman enhancement factor (EF) of the single Au@Ag NP-Au film junction is estimated by comparing the 1573 and 1585 cm^{-1} (ring stretching) peaks of the normal Raman scattering (I_{Raman}) of the BPT powder on the cover glass and the corresponding TERS signal (I_{TERS}) from the junction per number of probe molecule (N_{Raman} and N_{TERS}, respectively);

$$EF = \frac{I_{TERS}/N_{TERS}}{I_{Raman}/N_{Raman}}$$

The number of probe molecules for the normal Raman, N_{Raman}, is calculated to be 2.7×10^4 (N_{Raman} = [(density of BPT) × (diffraction limited area of the laser focal spot) × (depth of focus)] / (molecular weight of the BPT)). The number of BPT molecules for TERS, N_{TERS} is determined (N_{TERS} = (surface packing density of the BPT SAMs) × (area of the enhanced local field)). The value of packing density[1] is set to 4.25×10^{14} mol/cm^2. The area of the enhanced local field (A_{ELF}) is determined by the FDTD simulation results (see Figure S5, $A_{ELF} = \pi \times (\text{FWHM} / 2)^2$). For Au@Ag with diameters of 20, 30, 40, 50, and 60 nm, the FWHM is estimated to be 4.88, 5.60, 6.00, 6.58 and 6.96 nm, respectively.

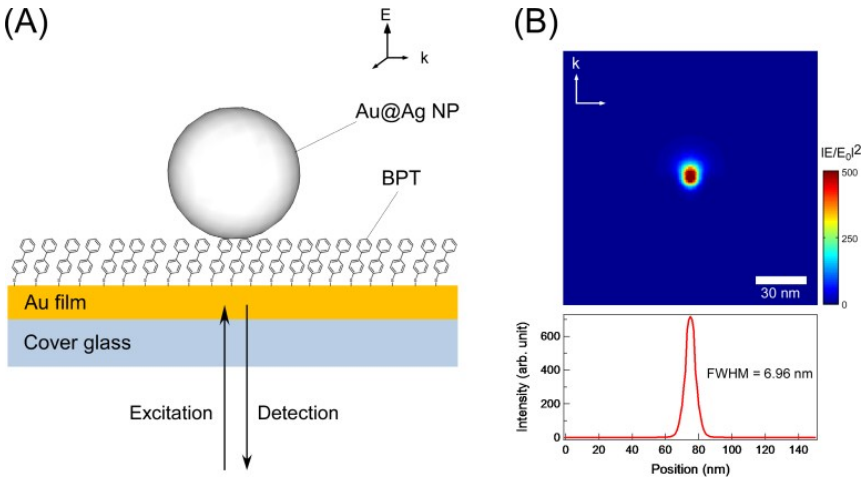

Figure S6. (A) Schematic diagram of the Ag@Ag NP-Au junction model. (B) Simulated electric field distribution in the xy-plane and the corresponding line-profile for Au@Ag NP (60 nm diameter) in near contact with Au thin film.

7. Finite-difference time-domain (FDTD) simulation of enhancement factors

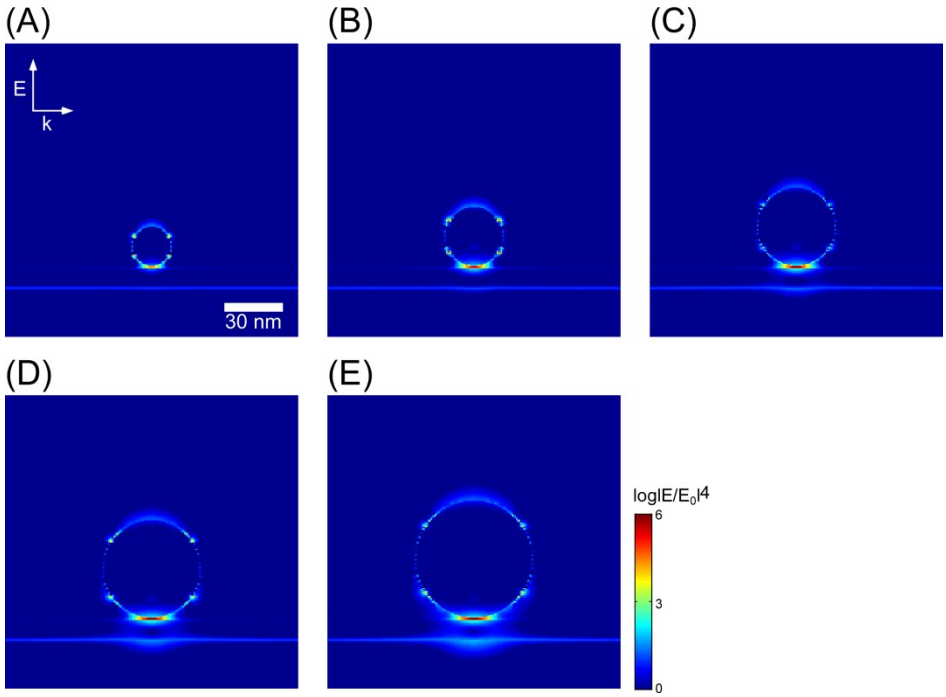

Figure S7. Simulated local field distribution between the 10-nm-thick gold film on a cover glass substrate and the Au@Ag NP with (A) 20 nm (B) 30 nm (C) 40 nm (D) 50 nm (E) 60 nm at λ = 532 nm. The spacing between gold film and Au@Ag NP is d = 1.25 nm, which accounts for the thickness of BPT SAM. The color scale representing the intensity is expressed in $\log |E/E_0|^4$.

8. Finite-difference time-domain (FDTD) simulation of AgNP

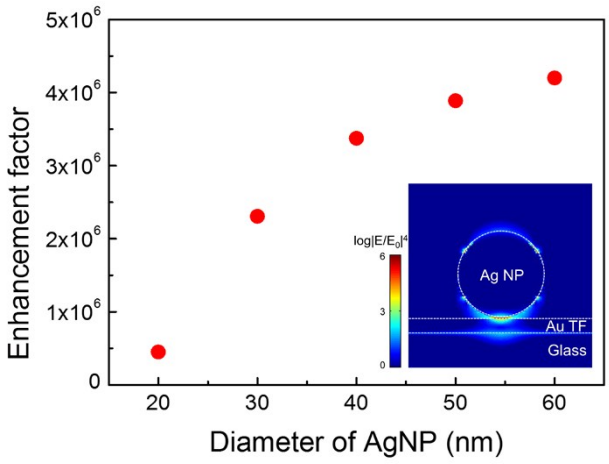

Figure S8. FDTD simulated enhancement factor calculated for AgNPs of various diameters in near contact with Au thin film (see inset image for the simulated local field enhancement, $|E/E_0|^4$, evaluated for AgNP with diameter of 60 nm).

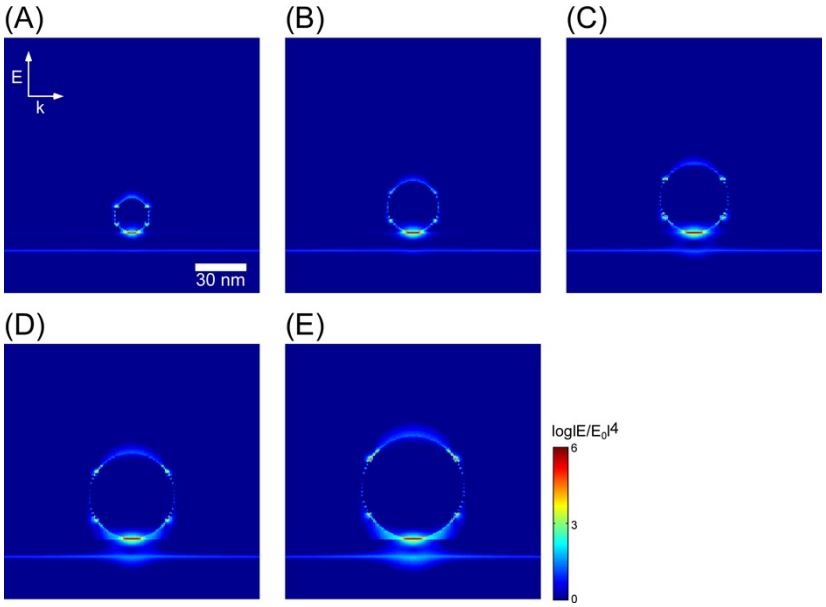

Figure S9. Simulated local field distribution between the 10-nm-thick gold film on a cover glass substrate and the AgNP with (A) 20 nm (B) 30 nm (C) 40 nm (D) 50 nm (E) 60 nm at λ = 532 nm. The spacing between gold film and AgNP is d = 1.25 nm. The color scale representing the intensity is expressed in log $|E/E_0|^4$.

9. Simulated spatial resolution of NP-tip as a function of the diameter of tip-end

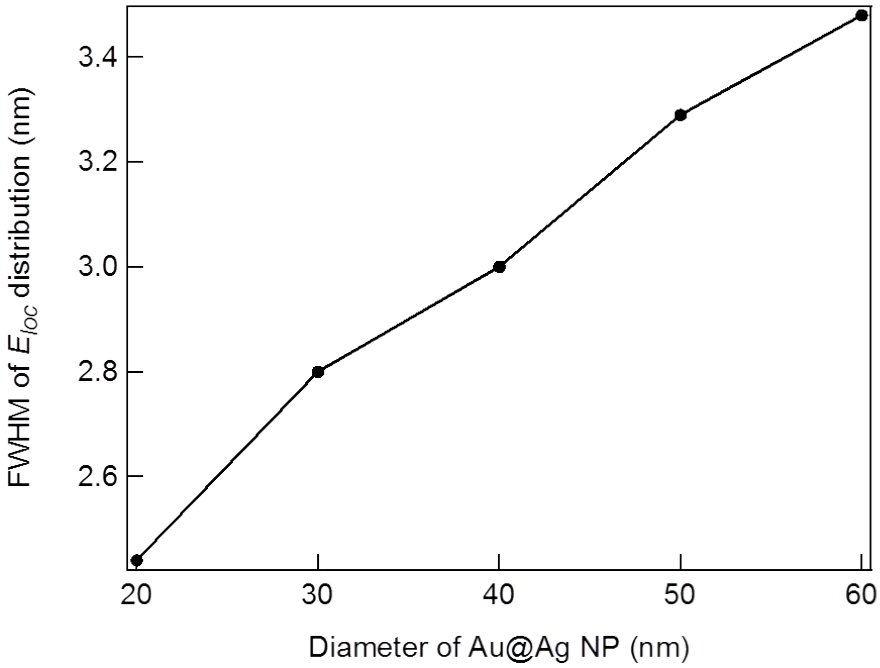

Figure S10. The change of spatial resolution as a function of the diameter of NP tip in TERS. The resolution is represented as the full-width at half-maximum of the local field intensity ($|E_{loc}/E_0|^2$) measured at the sample surface.

Table-S1. Peak assignment for Raman and TERS spectra for BPT[a] (in cm^{-1}). TERS peaks correspond to the measurement with Au@Ag NP-tip (diameter = 60 nm) based on refs. 2-4.

Peak No.	**Normal Raman[b]**	**TERS**	**Peak assignment[c]**
1		986.56	**δ(C-H)**
2	995	1003.4	
3		1020.3	
4	1103.8	1174.1	
5	1280.2	1288.3	ring **ν(C=C)**
6	1588.8	1573.3	
7	1592.6	1584.9	

a) All of the confocal Raman and TERS spectra were obtained with λ_{ex} = 532 nm.

b) The normal Raman spectrum was measured in solid (powder) state.

c) Refs. 2-4.

References

1. B. Bhushan and H. Liu, *Phys*. *Rev*. *B*, 2001, **63**, 245412.
2. J. Kalbacova, R. D. Rodriguez, V. Desale, M. Schneider, I. Amin, R. Jordan and D. R. Zahn, *Nanospectroscopy*, 2014, **1**, 12-18.
3. G. Socrates, Infrared and Raman characteristic group frequencies: tables and charts, *Ltd WJS*, 2001, 245.
4. Y. R. Lee, M. S. Kim and C. H. Kwon, *Bull. Korean Chem. Soc*., 2013, **34**, 470-474.